



HAL
open science

White-light supercontinuum generation in normally dispersive optical fiber using original multi-wavelength pumping system

Pierre-Alain Champert, Vincent Couderc, Philippe Leproux, Sébastien Février, Laurent Labonté, Vincent Tombelaine, Philippe Roy, Claude Froehly, Philippe Nerin

► To cite this version:

Pierre-Alain Champert, Vincent Couderc, Philippe Leproux, Sébastien Février, Laurent Labonté, et al.. White-light supercontinuum generation in normally dispersive optical fiber using original multi-wavelength pumping system. *Optics Express*, 2004, 12 (19), pp. 4366-4371. 10.1364/OPEX.12.004366 . hal-01657818

HAL Id: hal-01657818

<https://hal.science/hal-01657818>

Submitted on 3 Jan 2018

HAL is a multi-disciplinary open access archive for the deposit and dissemination of scientific research documents, whether they are published or not. The documents may come from teaching and research institutions in France or abroad, or from public or private research centers.

L'archive ouverte pluridisciplinaire **HAL**, est destinée au dépôt et à la diffusion de documents scientifiques de niveau recherche, publiés ou non, émanant des établissements d'enseignement et de recherche français ou étrangers, des laboratoires publics ou privés.

White-light supercontinuum generation in normally dispersive optical fiber using original multi-wavelength pumping system

Pierre-Alain Champert, Vincent Couderc, Philippe Leproux, Sébastien Février,
Vincent Tombelaine, Laurent Labonté, Philippe Roy and Claude Froehly

*Institut de Recherche en Communications Optiques et Microondes, UMR CNRS 6615
Faculté des Sciences et Techniques, 123 avenue Albert Thomas, 87060 Limoges Cedex, France
leproux@ircom.unilim.fr*

Philippe Nérin

ABX, Parc Euromédecine, Rue du Caducée, BP 7290, 34184 Montpellier Cedex 4, France

Abstract: We report on the experimental demonstration of a white-light supercontinuum generation in normally dispersive singlemode air-silica microstructured fiber. We demonstrate that the simultaneous excitation of the microstructured fiber in its normal and anomalous dispersion regimes using the fundamental and second harmonic signals of a passively Q-switched microchip laser leads to a homogeneous supercontinuum in the visible range. This pumping scheme allows the suppression of the cascaded Raman effect predominance in favor of an efficient spectrum broadening induced by parametric phenomena. A flat supercontinuum extended from 400 to 700 nm is achieved.

©2004 Optical Society of America

OCIS codes: (190.4370) Nonlinear optics, fibers; (190.1900) Diagnostic applications of nonlinear optics

References and links

1. *Optical Coherence Tomography and Coherence Techniques*, W. Drexler, ed., Proc. SPIE **5140** (2003).
2. R. R. Alfano and S. L. Shapiro, "Emission in the region 4000 to 7000 Å via four-photon coupling in glass," Phys. Rev. Lett. **24**, 584-587 (1970).
3. W. Yu, R. R. Alfano, C. L. Sam and R. J. Seymour, "Spectral broadening of picosecond 1.06 μm pulse in KBr," Opt. Commun. **14**, 344-347 (1975).
4. I. Ilev, H. Kumagai, K. Toyoda and I. Koprnikov, "Highly efficient wideband continuum generation in a single-mode optical fiber by powerful broadband laser pumping," Appl. Opt. **35**, 2548-2553 (1996).
5. W. Werncke, A. Lau, M. Pfeiffer, K. Lenz, H. J. Weigmann and C. D. Thuy, "An anomalous frequency broadening in water," Opt. Commun. **4**, 413-415 (1972).
6. P. B. Corkum, C. Rolland and T. Srinivasan-Rao, "Supercontinuum generation in gases," Phys. Rev. Lett. **57**, 2268-2271 (1986).
7. R. L. Fork, C. V. Shank, C. Hirlimann, R. Yen and W. J. Tomlinson, "Femtosecond white-light continuum pulses," Opt. Lett. **8**, 1-3 (1983).
8. C. Lin and R. H. Stolen, "New nanosecond continuum for excited-state spectroscopy," Appl. Phys. Lett. **28**, 216-218 (1976).
9. P. L. Baldeck and R. R. Alfano, "Intensity effects on the stimulated four photon spectra generated by picosecond pulses in optical fibers," J. Light. Technol. **5**, 1712-1715 (1987).
10. S. Coen, A. Hing Lun Chau, R. Leonhardt, J. D. Harvey, J. C. Knight, W. J. Wadsworth and P. St. J. Russell, "Supercontinuum generation by stimulated Raman scattering and parametric four-wave mixing in photonic crystal fibers," J. Opt. Soc. Am. B **19**, 753-764 (2002).

11. A. Mussot, T. Sylvestre, L. Provino and H. Maillotte, "Generation of a broadband single-mode supercontinuum in a conventional dispersion-shifted fiber by use of a subnanosecond microchip laser," *Opt. Lett.* **28**, 1820-1822 (2003).
12. B. Colombeau, J. Monneret, F. Reynaud, B. Carquille, F. Louradour and C. Froehly, "Réduction du gain de la diffusion Raman stimulée dans les fibres optiques unimodales de silice," presented at the Dixièmes Journées Nationales d'Optique Guidée, Jouy-en-Josas, France, Aug. 1989.
13. E. Golovchenko, E. M. Dianov, P. V. Mamyshev and A. N. Pilipetskii, "Parametric suppression of stimulated Raman scattering," *JETP Lett.* **50**, 190-193 (1989).
14. P. V. Mamyshev and A. P. Vertikov, in *Quantum Electronics and Laser Science*, Vol. 13 of OSA Technical Digest Series (Optical Society of America, Washington, D. C., 1992), p. 130.
15. S. Trillo and S. Wabnitz, "Parametric and Raman amplification in birefringent fibers," *J. Opt. Soc. Am. B* **9**, 1061-1082 (1992).
16. T. Sylvestre, H. Maillotte and E. Lantz, "Stimulated Raman suppression under dual-frequency pumping in singlemode fibres," *Electron. Lett.* **34**, 1417-1418 (1998).
17. S. Pitois, G. Millot and P. Tchofo Dinda, "Influence of parametric four-wave mixing effects on stimulated Raman scattering in bimodal optical fibers," *Opt. Lett.* **23**, 1456-1458 (1998).
18. P. Tchofo Dinda, S. Wabnitz, E. Coquet, T. Sylvestre, H. Maillotte and E. Lantz, "Demonstration of stimulated-Raman-scattering suppression in optical fibers in a multifrequency pumping configuration," *J. Opt. Soc. Am. B* **16**, 757-767 (1999).
19. T. Sylvestre, H. Maillotte, P. Tchofo Dinda and E. Coquet, "Suppression of stimulated Raman scattering in optical fibres by power-controlled multifrequency pumping," *Opt. Commun.* **159**, 32-36 (1999).

1. Introduction

Continuum generation has been widely studied in the past four decades due to the large potential applications such as telecommunications systems, time resolved absorption, spectroscopy, optical metrology or biomedical optics [1]. It was first demonstrated in bulk borosilicate glass [2] and later in a large variety of nonlinear media including liquid waveguides and gasses [3-6]. The progress and development in microstructured optical fibers brought a new range of fiber with manageable dispersion properties. The zero dispersion wavelength (ZDW) can thus be shifted toward the near IR and matched with the operating wavelength of a large variety of nanosecond to femtosecond high peak power lasers, yielding broadband continuum of more than 1000 nm at the -20 dB level [7-11]. Continuum generation is the result of multiple nonlinear phenomena such as stimulated Raman scattering (SRS), self-phase and cross-phase modulations (SPM and XPM), four wave mixing (FWM), high-order soliton formation and parametric mixing through modal phase matching in the case of multimode optical fibers. All these effects directly affect the continuum homogeneity and occur with different weights, according to the pump wavelength and power and to the chromatic dispersion characteristics of the fiber. Broadband continua were obtained by pumping a singlemode optical fiber near its ZDW or in regime of strong positive chromatic dispersion.

Nevertheless, no flat continuum generation has ever been demonstrated with large normal dispersion. Indeed in such conditions cascaded Raman scattering is the dominant effect and leads to an energy transfer from the pump towards discrete downshifted frequencies. To avoid the effect of SRS in optical fibers, several mechanisms have been suggested [12-16]. One of these mechanisms is based on a FWM process involving parametric Stokes and anti-Stokes sidebands and inhibiting the growth of the ordinary Raman Stokes radiation. Control of the Raman process was also investigated in high-birefringence fiber and demonstrated by means of a linearly-polarized dual-frequency pump scheme in the regime of strong positive dispersion where parametric suppression is not efficient [17-19].

In this paper, we report on the possibility to obtain a flat and homogeneous continuum in the visible range using a singlemode microstructured optical fiber (MOF) respectively pumped in its anomalous and normal dispersion regimes by the fundamental and second harmonic signals of a passively Q-switched nanosecond pulse laser. The double excitation allows the spectacular inhibition of the cascaded Raman process in favor of FWM and XPM, yielding a

white light supercontinuum source ranging from the near UV to the near IR (350-750 nm).

2. Experimental set-up with double pumping scheme

The set-up is shown on Fig. 1. The pump source consists of a passively Q-switch Nd:YAG laser operating at 5.4 kHz repetition rate and delivering 600 ps pulses at $\lambda = 1064$ nm. The free space radiation of the laser is frequency doubled in a 20 mm long type-II KTP crystal, with better than 35 % conversion efficiency, yielding pulses of 420 ps at $\lambda = 532$ nm. These IR and green radiations are coupled into a 4 m long MOF. Two filters (named "RG 85" and "BG 18") are used to allow total filtering of the visible or IR radiation at the launching end of the fiber.

The MOF used in these experiments has been fabricated in our laboratory by the conventional stack and draw process. A cross sectional scanning electron microscope image of the fiber is shown in Fig. 1. The hole-to-hole spacing Λ is around $2.2 \mu\text{m}$, leading to a core diameter approximately equal to $2.8 \mu\text{m}$. The average hole diameter d is $1.5 \mu\text{m}$. The resulting ratio d/Λ equal to 0.68 indicates that the fiber is slightly multimode. Indeed at the pump wavelengths of 1064 and 532 nm, we observed the guidance of LP_{01} and LP_{11} modes. Suppression of the second mode was achieved by coiling the fiber around a spool with a diameter of about 1 cm.

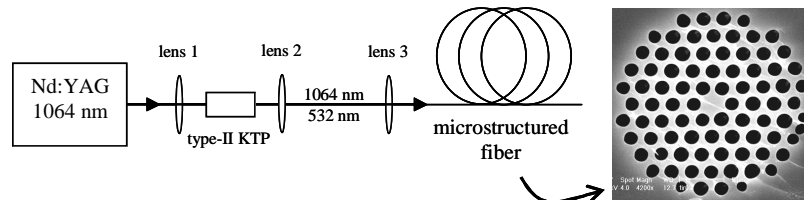


Fig. 1. Experimental set-up and cross sectional scanning electron microscope image of the microstructured air-silica fiber.

The chromatic dispersion and the effective area of the fundamental mode have been computed from 400 to 1600 nm using a full vectorial finite element algorithm and taking into account the actual cross section shown in Fig. 1. The results plotted in Fig. 2 show that the ZDW is located at $\lambda \sim 870$ nm, thus between the two pump wavelengths $\lambda = 532$ nm and $\lambda = 1064$ nm. The chromatic dispersion is respectively -410 ps/nm/km and $+55$ ps/nm/km at these wavelengths. The small effective area A_{eff} , calculated to be around $4 \mu\text{m}^2$ at 800 nm, gives a nonlinear coefficient $\gamma = 2\pi \cdot n_2 / \lambda \cdot A_{\text{eff}}$ equal to $0.06 \text{ W}^{-1} \cdot \text{m}^{-1}$ at this wavelength (n_2 being the nonlinear refractive index, $n_2 \sim 3 \times 10^{-20} \text{ m}^2 \cdot \text{W}^{-1}$). The transverse energy distribution of the fundamental mode computed at 800 nm is also plotted in inset of Fig. 2(a).

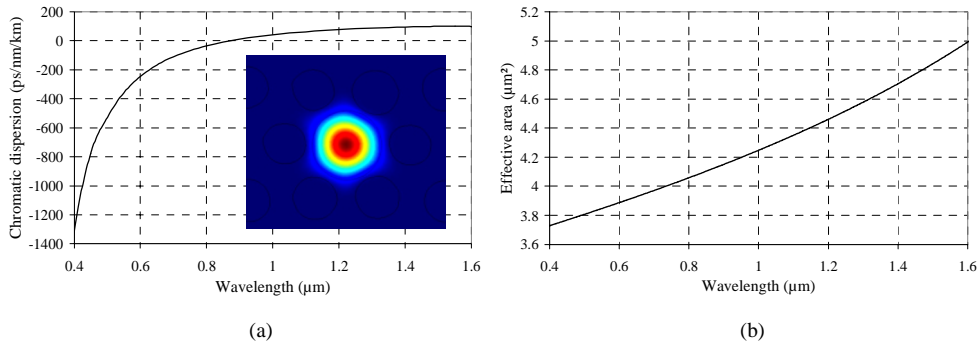


Fig. 2. Computed chromatic dispersion (a) and effective area (b) of the fundamental mode of the microstructured fiber versus the wavelength. Inset: transverse energy distribution calculated at $\lambda = 800$ nm.

3. Smooth and broadened supercontinuum generation

In a first case, the IR radiation is filtered out. The green peak power propagating in the waveguide is close to 1.5 kW for an average power of 3 mW measured at the fiber output. Due to the strong normal dispersion at 532 nm (-410 ps/nm/km), Raman scattering is the dominating nonlinear process. Indeed, up to seven Raman orders are generated through cascaded Raman effect (Fig. 3(a)).

We now consider the case when both the fundamental and second harmonic radiations are co-propagating in the fiber. The chromatic aberration of the coupling lens and the implementation of a longitudinal micro-displacement of the fiber allow a variation of the visible/IR power ratio coupled into the fiber core. For a sufficient power at 1064 nm, we observe a complete modification of the nonlinear behavior, giving birth to a symmetric and homogeneous broadening of the spectrum around 532 nm (Fig. 3(b)). This new continuum displays between 350 nm to 750 nm with a significant improvement of the spectrum flatness thanks to the quasi suppression of SRS effect. Except the remaining 532 nm peak, the 5 dB bandwidth has been measured to be close to 300 nm.

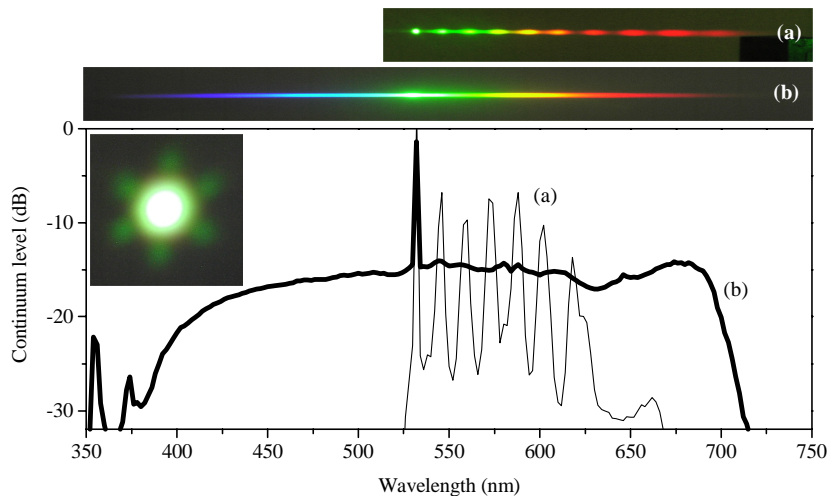


Fig. 3. Continuum generation in normal dispersion regime in the case of single (a) and dual (b) pump configuration. Pictures: diffracted beams. Graph: corresponding recorded power spectra. (a) The cascaded Raman effect is clearly visible in the presence of a single pump (532 nm). (b) The spectrum smoothly and symmetrically broadens when a second pump (1064 nm) is added. The corresponding singlemode transverse energy distribution is shown in inset (far field pattern).

The continuum can be divided into two parts. The first one at wavelengths larger than 532 nm seems to be obtained by the combination of FWM, SPM, XPM and SRS. In particular FWM and XPM are exacerbated by the presence of the second pump wavelength (1064 nm) situated in large anomalous dispersion regime ($+55$ ps/nm/km). Because of the high parametric gain, the SRS phenomenon is significantly reduced, allowing the growth of a continuous and flat spectral broadening. Nevertheless, the presence of some residual oscillations proves that the Raman effect is not completely suppressed and may still contribute to the broadening. The limit of the supercontinuum in the near infrared region (~ 750 nm) directly depends both on the green and IR pump powers. The higher the pump powers, the broader the supercontinuum.

In the second part (from 380 nm to 532 nm), the spectrum profile is particularly smooth without disconnections or oscillations. The wavelength growth seems to be built from the

combination of XPM and parametric effects. Indeed it seems that the spectral broadening obtained in the infrared region between 1064 nm and 1750 nm (see Fig. 4) has a role in the creation of wavelengths in the blue/UV region. Moreover no contribution of the SRS phenomenon is expected in this range of wavelengths, where anti-Stokes waves receive no significant energy. The limit of the supercontinuum in the blue range directly depends on the IR pump power and seems to be less sensitive to the green energy. Below 380 nm, only two peaks centered at 355 and 365 nm are identified and seem to be created by the third harmonic generation from the infrared pump.

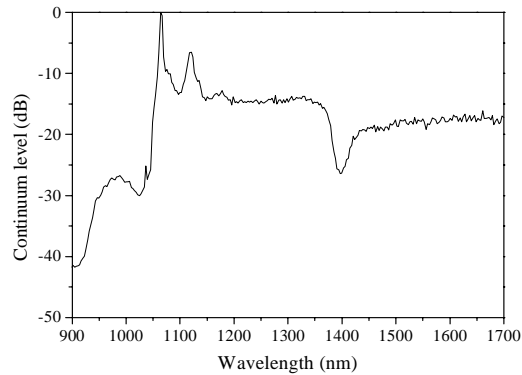


Fig. 4. Continuum power spectrum measured in the infrared range (anomalous dispersion regime).

It is worth to note that the change in the nonlinear process depends on the input IR pump power and on the power ratio $P_{\omega}/P_{2\omega}$ between 1064 nm and 532 nm pump wavelengths. In our experiments, the quasi complete suppression of the SRS phenomenon and the smoothing of the spectrum profile occurred notably for a ratio $P_{\omega}/P_{2\omega} > 2.8$. For a lower ratio, residual Raman peaks were clearly visible in the spectrum profile and no significant spectral broadening between 350 and 532 nm was observed (Fig. 5). In any case, the competition between FWM and SRS phenomena seems to be the right explanation of the continuum profile evolution.

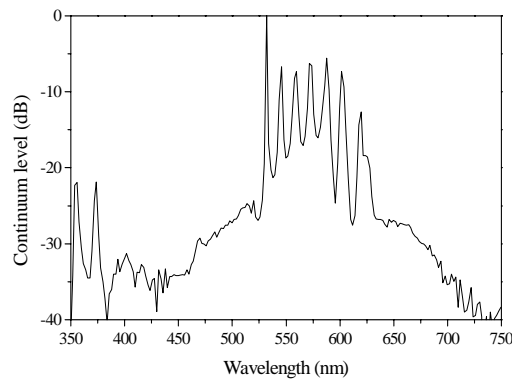


Fig. 5. Continuum power spectrum obtained in the visible range when using both 532 and 1064 nm pumps, but for an insufficient value of ratio $P_{\omega}/P_{2\omega}$.

The contribution of the 1064 nm pump is also visible in the infrared domain (Fig. 4). We observe a significant spectral broadening towards high wavelengths, reaching the upper limit of the optical spectrum analyzer used (1750 nm). The combination of SRS and FWM gives birth to a smooth spectrum profile. Unfortunately, the OH⁻ bonding present inside the MOF

silica core induces a significant absorption at $\lambda \sim 1.4 \mu\text{m}$, restricting the usable bandwidth of this infrared continuum in optical coherent tomography applications. Nevertheless, this drawback can be avoided when fabricating the MOF by using a non flame fused silica glass, exhibiting low OH^- absorption. An example of IR spectrum obtained in an OH^- -free MOF fabricated in our laboratory is shown in Fig. 6 and successfully confirms the necessity to use adequate silica material.

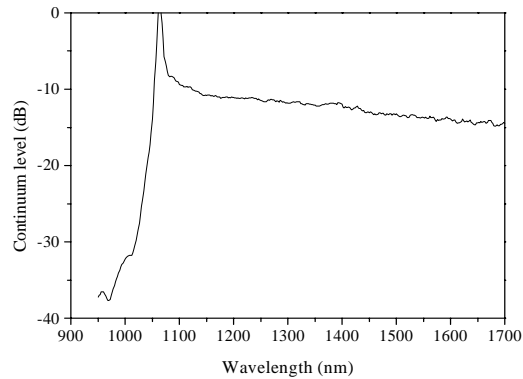


Fig. 6. Infrared continuum power spectrum obtained in a microstructured fiber fabricated at IRCOM with non flame fused silica glass. No more OH^- absorption peak is observable at 1400 nm.

4. Conclusion

We have demonstrated supercontinuum generation in normally dispersive air-silica microstructured optical fiber using a double pumping scheme with both 532 and 1064 nm radiations. A significant and symmetrical spectrum broadening due to the synchronic excitation in large normal and anomalous dispersion regimes was observed, resulting in a flat and homogeneous continuum between 400 and 700 nm. The addition of a second pump in the infrared range permitted to exacerbate the four wave mixing processes and to significantly inhibit the stimulated Raman scattering phenomenon. Thus a singlemode and truly white laser source was achieved. Wide spectral broadening over all the infrared range between 1064 and 1750 nm (upper limit of measurement device) was also obtained.

The new pumping scheme proposed here is applicable to all optical fiber in order to broaden and flatten the spectral continuum profile by the control of Raman effect. For example, it is possible to pump a standard singlemode fiber on both sides of its zero-GVD wavelength ($\sim 1300 \text{ nm}$) for supercontinuum generation in second and third communication windows. Moreover the multi wavelength pumping can be extended to three or four synchronic radiations, generated from an efficient laser source, to cover the whole transparency window of silica fibers.

In addition, we have recently fabricated in our laboratory a new microstructured fiber, whose well-adapted dispersion properties and low UV-absorption allow to efficiently improve the continuum generation below 380 nm, resulting in a quasi constant power level from at least 350 to 532 nm (without deteriorating the broadening beyond 532 nm). These results will soon be proposed for publication.

Acknowledgments

The authors thank ABX Diagnostics (HORIBA group) for financial support, J. L. Auguste and J. M. Blondy from IRCOM for the fabrication of the fibers, S. Coen (Auckland University), J. Dudley and T. Sylvestre (Université de Besançon) for fruitful discussions.